On the Balance between Model Detail and Experimental Information in Steam Methane Reforming on a Ni/MgO-SiO_2 Catalyst

Brigitte R. Devocht[1], Joris W. Thybaut[1*], Naoki Kageyama[2], Kenneth Toch[1], S. Ted Oyama[2,3*], Guy B. Marin[1]

[1] Ghent University, Laboratory for Chemical Technology, Ghent, B-9052, Belgium. *Email: joris.thybaut@ugent.be

[2] University of Tokyo, Department of Chemical System Engineering, 7-3-1 Hongo, Bunkyo-ku, Tokyo, 113-8656, Japan. *Email: oyama@vt.edu

[3] Virginia Polytechnic Institute and State University, Environmental Catalysis and Nanomaterials Laboratory, Blacksburg, VA, 24061-0211, USA.

* Corresponding authors

Abstract

The optimization and full understanding of chemical reactions is aided by the construction of an adequate kinetic model. The development of such a kinetic model remains a challenging task, especially for newcomers in the field. To tackle this challenge in the most efficient way an iterative, systematic methodology, originally demonstrated for *n*-hexane hydroisomerization, is now employed and further elaborated for methane steam reforming, focusing on identifying the balance between the level of detail accounted for by the model and the experimentally available information. The kinetic model is extended in a stepwise manner from a power law to a Langmuir-Hinshelwood-Hougen-Watson model accounting for reactant and product adsorption. The performance of the initially underparameterized model improved significantly by adding reactant adsorption, yet, including product adsorption led to overparameterization rather than enhanced model performance. Therefore, depending on the envisaged model application a correspondingly adequate amount of information is required for model development.

Acknowledgements:

This work was supported by a doctoral fellowship from the Fund of Scientific Research Flanders (FWO), the European Research Council under the European Union's Seventh Framework Programme (FP7/2014-2019) / ERS grant agreement n° 615456 and the 'Long Term Structural Methusalem Funding by the Flemish Government'. This work was also supported by the Japan Science and Technology Agency under the CREST program, Grant Number JPMJCR16P2. JWT acknowledges the ERC for the PoC grant SERENiTi (GA n° 825783).

Introduction

The development of new chemical processes and the intensification of existing ones strongly benefits from a thorough understanding of the various phenomena occurring on the different relevant scales. Kinetic modeling constitutes an essential central link between those scales and allows acquiring insight in the underlying reaction mechanism that steers the overall process [1-3]. Nevertheless, kinetic model development remains challenging because it requires expertise which is not easily transferred via textbooks. A proper balance should be identified between the level of detail accounted for in the model and the information available from potentially expensive experiments [4]. The exact location of this balance may depend on the ultimately anticipated use of the model, ranging from process control purposes to studies for fundamental insight. Moreover, when the kinetically relevant reactions and species change significantly with changing operating conditions or conversion, a microkinetic assessment is recommended, while in other cases a more simple model may be sufficient.

The higher the degree of detail in the model, the more extensive the data set needs to be. It goes without saying that reaching a high performant microkinetic model with a clear physical meaning requires significant expert involvement. Know-how to construct the microkinetic

model and acquire an extended, dedicated experimental data set at varying operating conditions is crucial. Dealing properly with the less dominant pathways accounted for in the network and the large degree of freedom typically encountered in those models may pose specific challenges, while a standard reaction analysis with one or several rate-determining steps and equilibrated reactions can still give a physically realistic description. Moreover, the microkinetic analysis does not give a closed-form rate expression making its use in reactor design less straightforward [5,6].

A systematic methodology is required to guide the model developer towards the balance between the amount of information available and the degree of model detail, and the corresponding adequate kinetic model. Toch et al. [7] proposed a procedure which allows the kinetic modeler to reach the optimal balance between statistical significance and physical meaning with the least effort. In this work, an additional dimension will be added to the methodology, which additionally takes the balance between available information and model detail into account. The focus will be on the iterative nature of the extended methodology and the refinement of the model based on insight obtained in previous iterations, within one direction of the added dimension, i.e., the direction of enhanced model detail.

The methodology is demonstrated via a case study of steam methane reforming (SMR). SMR is, worldwide, the major and most cost-effective industrial route for hydrogen production from natural gas [8,9]. Being the simplest, lightest and most abundant element in the universe, hydrogen can be regarded as a promising energy carrier for future generations [10,11]. SMR accounts for 50 % of the global hydrogen production and has thermal efficiencies up to 85 % [12]. It is a mature technology that converts methane and steam at sufficiently elevated temperatures, i.e., 900 – 1300 K and pressures, i.e., 0.3 – 2.5 MPa into synthesis gas. Typical inlet molar steam to carbon ratios vary between 3:1 and 5:1. The operating conditions are tuned depending on the end-use of the outlet gas. High heat fluxes are required for the strongly endothermic reforming

reaction. The equilibrium limited SMR process is typically operated in a packed bed reactor with recycle to achieve higher efficiencies. Ni catalysts are industrially most commonly employed for this reaction because of their low cost and comparable activity to noble metals [13]. Nevertheless, the development of new, stable catalysts remains a very active research field [12,13].

Stoichiometrically, SMR can be described by two reactions, i.e., the strongly endothermic reforming of methane, (1), and the moderately exothermic water-gas shift (WGS) reaction, (2).

$$CH_4 + H_2O \rightleftharpoons CO + 3H_2 \qquad \Delta H^0_{298} = 206.1\,\text{kJ mol}^{-1} \qquad (1)$$

$$CO + H_2O \rightleftharpoons CO_2 + H_2 \qquad \Delta H^0_{298} = -41.1\,\text{kJ mol}^{-1} \qquad (2)$$

Since the 1950s, significant efforts have been devoted to the understanding of the reaction mechanism and the construction of the corresponding rate expressions for SMR [14]. It is generally accepted that methane reforming proceeds via a complex mechanism comprising several parallel and consecutive steps. Various alternative mechanisms have been suggested with different degrees of detail and varying assumptions, e.g., concerning the role of water as co-reactant. An overview of some of the most important SMR studies is presented in the state-of-the-art section. The general form of SMR rate expressions reported in literature is shown in Eq.1 [15,16].

$$r_1 = k\, p_{CH_4} \frac{f\left(p_{H_2O}, p_{H_2}\right)}{\left(1+g\left(p_{CH_4}, p_{H_2O}, p_{H_2}, p_{CO}, p_{CO_2}\right)\right)}\left[1-\frac{p_{CO}p^3_{H_2}}{p_{CH_4}p_{H_2O}K_{SMR}}\right] \qquad \text{Eq.1}$$

To demonstrate the iterative identification of the adequate balance between available information and detail accounted for in the model, a kinetic model for the SMR data acquired over a Ni/MgO-SiO_2 catalyst in a packet bed reactor is proposed. The aim is to construct rate expressions which can adequately describe the experimental data, satisfying both statistical significance and physical meaning and identifying the degree of model detail which is in balance with the information contained within the data. To do so, the model is extended in a stepwise manner, starting from a global power law model towards more complex, physically

relevant models, e.g., a Langmuir-Hinshelwood-Hougen-Watson (LHHW) model. The iterative methodology is applied until no further improvements in model performance are obtained and the model would tend to become overparameterized [17].

Procedures

1. Experimental data

Steam Methane Reforming (SMR) was investigated on a Ni/MgO-SiO_2 catalyst, supplied by JGC Catalysts and Chemical Ltd. While Ni is the most frequently employed metal for reforming, the magnesium silicate support has not been investigated extensively. It is a low cost material and exhibits a high strength and sulfur resistance. It allows more easy reduction than Al_2O_3-based supports. All of these advantages make a more extended kinetic investigation of the performance of Ni deposited on the MgO-SiO_2 support worthwhile. In total, 36 experiments, including 14 repetition experiments, were performed in a packed bed reactor, see Figure 1. The total pressure in the reactor was kept at 400 kPa and the partial pressure of the reactants, methane and water, was varied between 20-140 kPa and 80-320 kPa respectively, with N_2 as inert. The temperature was fixed at 923 K. The outlet gases methane, carbon monoxide and carbon dioxide, were separated from the water and analyzed by a gas chromatograph with a TCD detector. The carbon balance was closed within 7 % for all experiments. The outlet molar flow rates of water and hydrogen were determined by also closing the oxygen and hydrogen mass balances. No catalyst deactivation was observed during the experimental campaign. The setup is operated in the intrinsic kinetics regime and, hence, the observed reaction rates are nor limited nor biased by any transport or hydrodynamic phenomena [18,19]. A full description of the experimental setup, the operating conditions and the catalyst can be found in previous work [18].

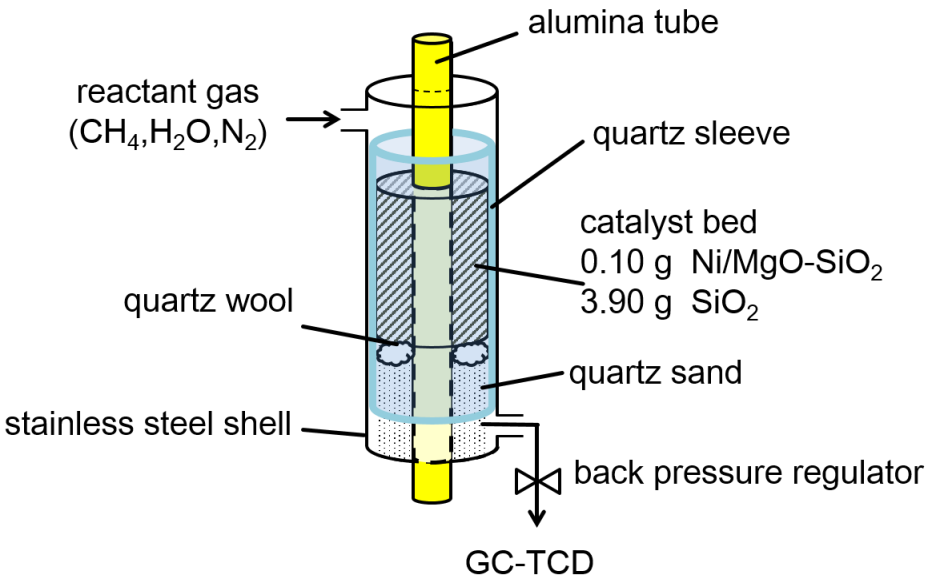

Figure 1. Schematic representation of the reactor used for steam methane reforming.

The well-defined amount of information in the data set makes this case study an interesting and real-life example. Researchers often have access to a rather limited data set from literature or from an expensive experimental campaign, for example in collaboration with a third party. They are challenged to extract as much information as possible from the data as required for their application to build the model, the acquisition of additional experimental information not being evident.

The main trends in the experimental data set have already been discussed more extensively elsewhere [18] and are only briefly summarized here. The methane conversion increases with decreasing methane inlet partial pressure, i.e., from 120 kPa to 40 kPa, and increasing water inlet partial pressure, i.e., 80 kPa to 240 kPa. Only at the highest water inlet partial pressures, i.e. 280 kPa and 320 kPa, the conversion decreases again, indicating the presence of competitive adsorption between methane and water. At high water partial pressures, methane adsorption on the catalyst surface is hindered, since dissociative water adsorption on the catalyst surface is relatively more pronounced at the temperatures considered in this work [14]. The selectivity to carbon monoxide and carbon dioxide respectively decreases from 33 % to 18 % and increases

from 67 % to 82 %, with increasing water inlet partial pressure, i.e., from 160 kPa to 280 kPa, and exhibites only a minor dependence on the methane conversion.

The affinity A (-ΔG) of the overall reactions (1) and (2) is calculated to determine in which direction these reactions proceed at the reactor outlet [20], which will be useful for the kinetic model development. As a rule of thumb, global reactions with an affinity |A| lower than 10 kJ mol^{-1} can be assumed to be close to equilibrium. The affinity |A| of the methane reforming and the WGS step vary between 15 and 50 kJ mol^{-1} and -3 and 2 kJ mol^{-1} respectively. It is evident that the reforming reaction (1) is far from equilibrium and proceeds in the forward direction at the reactor outlet, while the WGS reaction (2) is close to equilibrium at the reactor outlet.

2. Definitions and calculation of quantities and responses

The methane conversion, X_{CH_4}, is defined as the ratio of the methane amount consumed by reaction and the initial amount fed to the reactor, see Eq.2, with $F^0_{CH_4}$ and F_{CH_4} the methane inlet and outlet molar flow rates.

$$X_{CH_4} = \frac{F^0_{CH_4} - F_{CH_4}}{F^0_{CH_4}} \qquad \text{Eq.2}$$

The selectivity towards carbon monoxide and carbon dioxide, generally represented as component j, from methane is presented by Eq.3, with F_j the outlet molar flow rate of component j.

$$S_j = \frac{F_j}{F^0_{CH_4} - F_{CH_4}} \qquad j = CO \text{ or } CO_2 \qquad \text{Eq.3}$$

In this work, the space time is defined by the ratio of the catalyst mass W and the inlet molar flow rate of methane, see Eq.4.

$$\text{space time} = \frac{W}{F^0_{CH_4}} \qquad \text{Eq.4}$$

3. Kinetic modeling and regression

The model parameters have been determined by regression against experimental data via the application of the iteratively reweighted least squares (IRLS) method [21]. This method minimizes the weighted sum of squares of the residuals e, approximating the experimental error ϵ, see Eq.5, with respect to the model parameters β, see Eq.6. To account correctly for the potential heteroscedasticity of the experimental error between the responses, i.e., the error variance not being independent of the operating conditions, the elements of the sum of squares are weighted by the variance-covariance matrix $\underline{V}$ [2,7,22].

$$\underline{e} = \underline{f}(\underline{X}, \underline{b}) - \underline{y} \qquad \text{Eq.5}$$

$$S(\underline{\beta}) = \underline{\varepsilon}^T \underline{V}(\underline{\varepsilon})^{-1} \underline{\varepsilon} \xrightarrow{\underline{\beta}} \min \qquad \text{Eq.6}$$

The considered model responses ($\underline{y}$) are the outlet molar flow rates of the components methane, carbon monoxide and carbon dioxide. The molar flow rate of water and hydrogen are calculated based on elementary balances and the three experimentally observed responses. The temperature, total pressure, space time and inlet composition constitute the independent variables $\underline{X}$ [18].

The packed bed reactor is described as a steady-state, ideal plug flow reactor. A mass balance over the reactor for each component leads to a set of differential equations, see Eq.7, with R_j the net rate of formation of component j.

$$dF_j = -R_j dW \qquad F_j(W=0) = F_j^0 \qquad \text{Eq.7}$$

The regression results are assessed in various ways, e.g., via parity diagrams, performance curves, residual figures and normal probability plots. The statistical dependence of the parameters is verified through the binary correlation coefficients [7]. The higher the coefficient, the more correlated both parameters are. However, only if the absolute value of the binary correlation coefficient exceeds 0.95, the parameters are considered to be correlated. The global significance of the regression is assessed via an F test based on the hypothesis that all

parameters would simultaneously be equal to zero. Another F test is used to determine the model adequacy by verifying whether the difference between the experimentally observed responses and the model calculated responses can be mainly attributed to the experimental error or whether a systematic deviation would be involved. It should be noted that the latter F test is a severe test, which is rarely fulfilled. A more theoretical background and the corresponding formulas of both tests can be found elsewhere [7,18].

In order to perform the actual model construction, regression and statistical analysis in a more automated manner, the microKinetic Engine (μKE) was used. The μKE is a user-friendly and flexible, kinetic modeling and regression software package, which has been developed at the Laboratory for Chemical Technology at Ghent University [23]. The Rosenbrock and Levenberg-Marquardt algorithms are successively applied in the μKE to determine the most optimal parameter estimates $\underline{b}$ and their confidence interval. To further increase the user flexibility, the μKE has been extended with user defined functions, allowing the μKE to handle any user defined model both with chemical and non-chemical applications.

4. State-of-the-art of kinetic models

The literature about SMR is comprehensive and kinetic models ranging from power law models to detailed microkinetic models have been developed over the last half-century. The investigated catalysts and operating conditions vary widely and most of the developed rate expressions are only valid within a limited range of experimental conditions. In this section an overview will be given of the most important kinetic models proposed in literature from the point of view of model development with a focus on the varying complexity of the models.

The most simple kinetic models for SMR are the **power laws**, in which no surface species are explicitly taken into account. Power law models are proposed, among others, by Akers et al. [24], Saito et al. [25] and Wang et al. [26], see Table S1 in the Supplementary Material. Most, but not all,

researchers found a first-order dependence on methane for the methane consumption for different catalysts in a broad range of experimental conditions. This finding also extends towards the more complex models which will be discussed further [14,16,24,27-32]. This indicates that the rate-determining step effectively consumes one methane molecule. Moreover, literature shows that the co-reactant water does not have any kinetically relevant role, and, hence, the reaction rate is independent of, i.e., zero order in, the water content [24,27,29-31]. Other authors state that both reactants, methane and water, affect the methane consumption rate for an extended range of conditions and for different catalysts [14,25,26,33-35]. Also for the WGS reaction, variations with respect to the partial reaction orders of the components are proposed. For example, some investigations indicated that the WGS rate is zero order in carbon monoxide and first order in water on a Rh catalyst [29], while others claim it has a first-order dependence on carbon monoxide and half-order dependence on water on a Ni catalyst [14] and Rh catalyst [31]. Power law models do not account for catalyst interaction, yet, they can provide useful information with respect to, e.g., adsorption phenomena, based on variations of the partial reaction orders with independent variables.

Researchers such as Numaguchi et al. [33] and Tonkovich et al. [36], see Table S1 in the Supplementary Material, went one step further and included reversibility in their **power law models**. The models remain empirical, but the resulting **driving force** in the rate expressions takes potential equilibrium constraints into account.

The next group of kinetic models for SMR are categorized in this work as the **LHHW models**. The models comprise a kinetic, a driving force and an adsorption term, albeit sometimes in a modified form [20]. Some highly cited examples are the models proposed by Bodrov et al. [37], Khomenko et al. [34], Xu and Froment [38], Soliman et al. [39] and Hou and Hughes [14], see Table S1 in the Supplementary Material. In these models it is typically assumed that, to a certain extent, hydrogen can inhibit the reaction rate [40]. Hydrogen co-feeding is frequently performed to avoid

catalyst deactivation by reoxidation and carbon deposition [41,42]. The feed of an industrial reformer generally also contains hydrogen for example due to recycle streams [14,42]. Due to the presence of hydrogen in the feed, no numerical issues are encountered, i.e., the calculated reaction rate tending towards infinity in case of reduced hydrogen availability, when employing these kinetic models.

The final and most detailed type of model is the **microkinetic model**, e.g., Aparicio [40], Maestri et al. [29] and Sprung et al. [35] in Table S1 in the Supplementary Material. A large thermodynamic and kinetic database and/or regression against a sufficiently extended experimental data set is required to justify this level of detail.

Balancing experimental and model design to avoid underparameterization and overparameterization

The systematic methodology of Toch et al. [7] is extended by including a new dimension related to the balance between the amount of information available and the degree of model detail aimed at. Insight is typically gained from time-consuming and expensive experiments, such as high throughput kinetics determination [43] and catalyst characterization. In addition, quantum chemical calculations can provide further insight into the mechanism [44]. Depending on the envisaged level of model detail, i.e. from a global model towards a microkinetic one, a minimum amount of information exists which is needed for model development. Complex models obviously require an extensive data set, while for global models a more limited data set suffices. Generally kinetic models which take more details into account and explicitly account for reactions at the elementary level, have a better performance in describing the mechanism [45], yet a microkinetic analysis is not always required. It is not uncommon that only a limited number of reactions and species significantly contribute to the overall reaction [46,47]. The inclusion of irrelevant elementary steps makes the determination of the corresponding

parameters very challenging, not to say, impossible. In this case, the microkinetic model will spontaneously reduce itself to a more simple one.

The goal is to construct the model aimed at with minimum effort and cost, i.e., based on this minimum amount of information which is needed for model development. The experimental data set is the subject of the first step of every iteration within the systematic methodology. Performing experiments in an intelligent manner, for example through experimental design, increases the insight in and knowledge about the reaction mechanism of interest. This corresponds to a vertical movement in the information vs model detail plane, see Figure 2. The development of the kinetic model is the second step within the methodology. The expansion or reduction of the model corresponds to a horizontal movement.

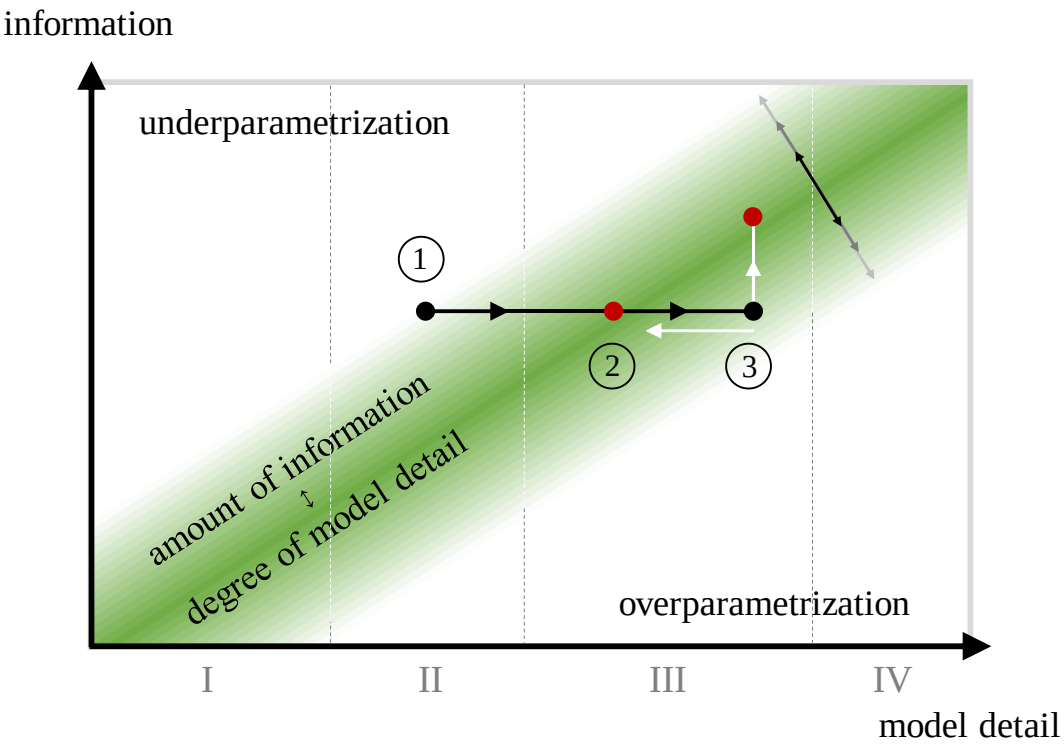

Figure 2. Schematic representation of the balance between information and model detail. Zones with different model complexity: I = power law, II = power law with driving force, III = LHHW, IV = microkinetic. Models case study SMR: 1 = Numaguchi model, 2 = model with reactant adsorption, 3 = LHHW model.

Two zones can be identified: the zone of underparameterization and the zone of overparameterization. The right balance between the available knowledge and the degree of detail is situated on the boundary between both regions, see Figure 2. The latter, green border should be aimed at in order to obtain an adequate model with minimum effort, nevertheless, even within the balanced zone some variation exists. The broadness of the green boundary and the preferred position thereon depend on the goal to be achieved thanks to the model and the available resources.

An underparameterized model lacks essential features to describe the investigated reaction. The effect of one or more independent variables on the model response is not correctly accounted for. Hence, the model simulated values typically exhibit band formation, i.e., show limited variation as a function of the independent variable(s), in the parity diagrams, performance figures and residual figures [16,48]. When the model complexity is too high for the information contained within the experimental data set, an overparameterized model is obtained. Overparameterization leads to non-significant model parameters, which have no clear physical meaning and are highly correlated [16,48]. A strategic extension of the experimental data set, e.g., via experimental design techniques, or adaptation of the degree of detail accounted for in the model, allows the modeler to move from the zone of underparameterization or overparameterization towards the balanced zone in the horizontal or vertical direction, see white arrows in Figure 2. A posteriori techniques for discrimination between rival models can also be convenient when multiple models/model assumptions are considered.

The roman numbers I to IV in Figure 2 indicate zones of varying model complexity, i.e., power law models, power law models with a driving force, LHHW models and microkinetic models, in correspondence with the types of models discussed in the State-of-the-art of kinetic models. The four zones also correspond to different types of data required for model development, i.e.,

a limited data set will typically suffice for power law models, while quantum chemical calculations and advanced characterization techniques are required for microkinetic modeling.

The extended methodology is applied for the development of a kinetic model for the SMR over a N/MgO-SiO_2 catalyst. The goal is to establish an adequate model, which exhibits both statistical significance and physical relevance and which is in balance with the information contained within the experimental data. The experimental campaign has been completed a priori and, therefore, the experimental information available remains constant during the model development, see vertical axis in Figure 2. The degree of detail of the model will be stepwise expanded during each iteration, see horizontal axis in Figure 2.

Application of the systematic methodology on SMR

1. Base case

Description and construction

The systematic methodology starts with the acquisition and analysis of the experimental data and a literature survey. The present data set indicates that the reversibility of the considered reactions has to be accounted for to correctly describe the WGS reaction and that competitive adsorption between the reactants may play an important role, see Procedures. The literature survey yielded a large number of potential kinetic models. Since the information contained within the experimental data set is relatively limited and the aim of this work is to determine an adequate kinetic model describing the detail contained in this data set, a power law model is selected to start the model development. The model is shown as alternative ① in Figure 3, which displays the different stages of the model development for this case study. The reforming reaction (3) and WGS reaction (4), which are at the basis of this model, are shown in Table 1. The WGS reaction is implemented to be reversible based on the thermodynamic analysis of the

data set and for the sake of generality, the reverse reforming step, i.e., methanation, is also included in the model.

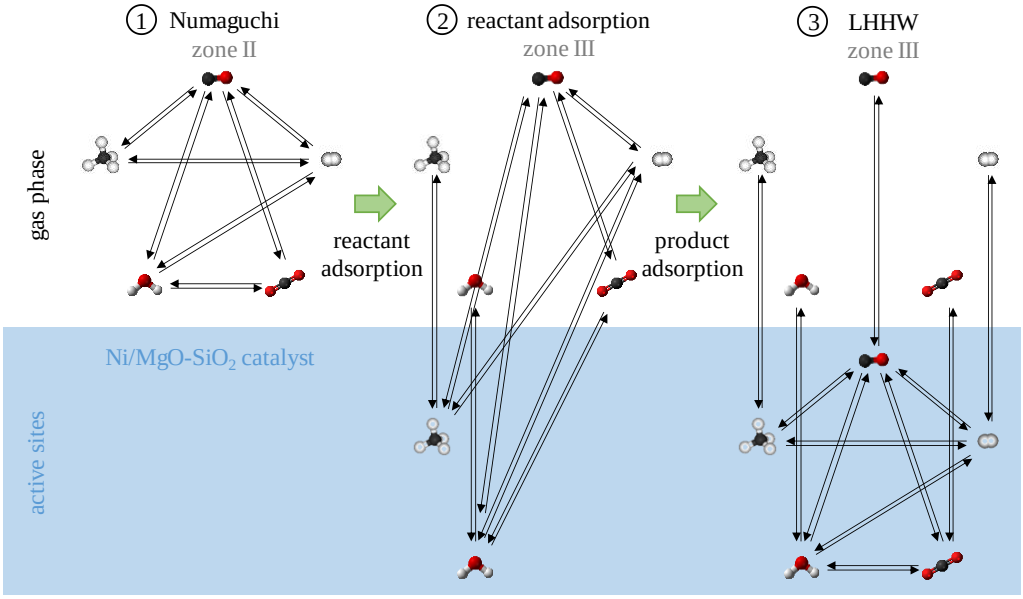

Figure 3. Model development for steam methane reforming. Zones with different model complexity: II = power law with driving force, III = LHHW.

Table 1. Reactions included in the Numaguchi model, the model with reactant adsorption and the LHHW model for SMR. Vacant active sites and adsorbed species are indicated with a star.

① Numaguchi model		③ LHHW model	
$CH_4 + H_2O \overset{k_1}{\rightleftharpoons} CO + 3H_2$	(3)	$CH_4 + * \overset{k_1}{\rightleftharpoons} CH_4^*$	(9)
$CO + H_2O \overset{k_2}{\rightleftharpoons} CO_2 + H_2$	(4)	$H_2O + * \overset{k_2}{\rightleftharpoons} H_2O^*$	(10)
② Model with reactant adsorption		$CH_4^* + H_2O^* + 2\,* \overset{k_3}{\rightleftharpoons} CO^* + 3\,H_2^*$	(11)
$CH_4 + * \overset{k_1}{\rightleftharpoons} CH_4^*$	(5)	$CO^* + H_2O^* \overset{k_4}{\rightleftharpoons} CO_2^* + H_2^*$	(12)
$H_2O + * \overset{k_2}{\rightleftharpoons} H_2O^*$	(6)	$CO^* \overset{k_5}{\rightleftharpoons} CO + *$	(13)
$CH_4^* + H_2O^* \overset{k_3}{\rightleftharpoons} CO + 3\,H_2 + 2\,*$	(7)	$CO_2^* \overset{k_6}{\rightleftharpoons} CO_2 + *$	(14)
$CO + H_2O^* \overset{k_4}{\rightleftharpoons} CO_2 + H_2 + *$	(8)	$H_2^* \overset{k_7}{\rightleftharpoons} H_2 + *$	(15)

The kinetic model of Toru Numaguchi and Katsutoshi Kikuchi, see State-of-the-art, is one of the most widely accepted global kinetic models for SMR [33,49]. The model is a power law model

with a thermodynamic driving force, see Eq.8 and Eq.9, and is, hence, selected for the initial model development.

$$r_1 = \frac{k_1^{comp}\left(p_{CH_4}p_{H_2O} - \frac{p_{CO}p_{H_2}^3}{K_{SMR}}\right)}{p_{CH_4}^{\alpha_1}\, p_{H_2O}^{\delta_1}} \text{ with } k_1^{comp} = \frac{k_1}{K_{H_2O}^m} \qquad \text{Eq.8}$$

$$r_2 = \frac{k_2^{comp}\left(p_{CO}p_{H_2O} - \frac{p_{CO_2}p_{H_2}}{K_{WGS}}\right)}{p_{CH_4}^{\alpha_2}\, p_{H_2O}^{\delta_2}} \text{ with } k_2^{comp} = \frac{k_2}{K_{H_2O}^m} \qquad \text{Eq.9}$$

α_1 and δ_1 allow tuning the partial reaction orders of methane and water in the reforming reaction, while α_2 and δ_2 allow the same in the WGS reaction. k_1^{comp} and k_2^{comp} are composite rate coefficients, which are interpreted as the ratio of the forward rate coefficient and the adsorption equilibrium coefficient of water to the power m, m being the number of active sites included in the rate-determining step [33]. K_{SMR} and K_{WGS} are the equilibrium coefficients of the global reforming (3) and WGS reaction (4) [50]. The equilibrium coefficients K_{SMR} and K_{WGS} are calculated based on NASA polynomials. The kinetic model of Numaguchi et al. is also referred to as the *Numaguchi model* in the remainder of this work.

Model and parameter estimates assessment and discussion

The regression was found to be globally significant with a calculated F_s value of $7.83\ 10^3$ ($F_{s,tab}$ = 2.66). The power law model tends to be inadequate, however, ($F_{a,calc}$ = 2.89 > $F_{a,tab}$ = 1.49), as will be further illustrated by the model performance in Figure 4.

The parameter estimates and the 95 % confidence intervals are shown in Table 2. The true partial reaction orders of methane and water in the reforming step are, respectively, 1- α_1 (=0.37) and 1- δ_1 (=0.13). The partial reaction order of methane of 0.37, in contrast to the literature value of one, might indicate that missing features in this model, such as competitive adsorption, are compensated for by lowering the methane partial reaction order, or that the

particular type of catalyst support leads to a reaction mechanism different from those reported in the literature. The low partial reaction order of water, with a rather broad confidence interval, confirms the limited impact of water on the reforming step.

The parameters α_2 and δ_2 are redundant to the model, i.e., the corresponding t values for their individual statistical significance were below the tabulated value and, hence, are sequentially eliminated from the model [21]. This is in accordance with the work of Numaguchi et al., where α_2 and δ_2 were also found to be statistically insignificant. The composite rate coefficient k_2^{comp} cannot be significantly estimated either, which indicates that in a significant part of the reactor, the WGS reaction brings very limited kinetic information. Hence, k_2^{comp} is fixed at a value of 2.53 10^{12} mol s^{-1} kg^{-1} $MPa^{\alpha 2+\delta 2-2}$, which is the minimum value required to establish the WGS equilibrium close to the reactor inlet. This is in agreement with the thermodynamic analysis, which indicated that the WGS reaction is very close to equilibrium. The model parameters are uncorrelated as the maximum binary correlation coefficient is equal to 0.82.

Table 2. Parameter estimates and the corresponding 95 % confidence intervals for the Numaguchi model. * = parameter was kept fixed during regression.

	95 % confidence interval	units
k_1^{comp}	1.09 ± 0.37	$10^5\,mol\,s^{-1}\,kg^{-1}\,MPa^{\alpha_1+\delta_1-2}$
k_2^{comp}	2.53*	$10^{12}\,mol\,s^{-1}\,kg^{-1}\,MPa^{\alpha_2+\delta_2-2}$
α_1	0.633 ± 0.050	-
δ_1	0.873 ± 0.069	-
α_2	0*	-
δ_2	0*	-

Residual analysis

The Numaguchi model, see Figure 4 top, is not capable of simulating the maximum in methane conversion and significantly overestimates the conversion at the lowest methane inlet partial pressures combined with the higher water partial pressures. The conversion increases only

slightly with increasing water inlet partial pressure, i.e., shows horizontal band formation, rather than the experimentally observed decrease in the performance figure, see blue line in Figure 4. As the discrepancy between experimentally observed values and model simulations cannot be attributed to the experimental error only, the model was considered to be inadequate, not only based on statistical grounds, but also on physico-chemical grounds. The interaction between the reactants and the catalyst is not explicitly considered in this simple power law model and competitive adsorption effects, as required to reproduce the effect of water on the methane conversion, are missing.

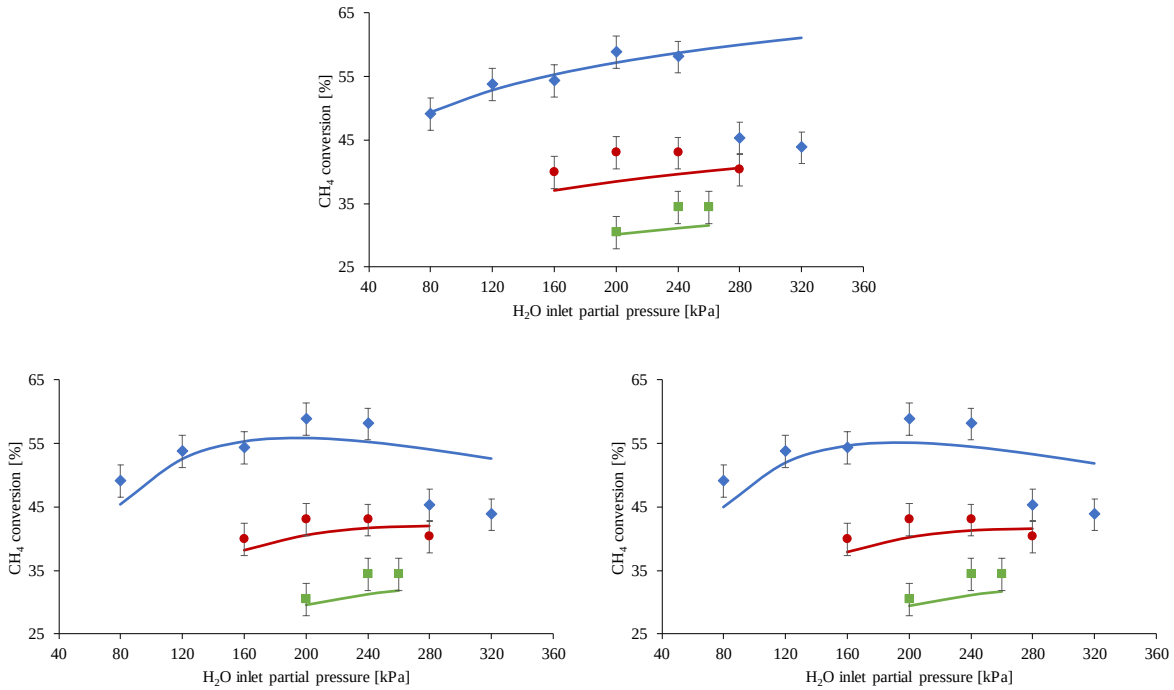

Figure 4. Methane conversion as a function of the water inlet pressure at a total pressure of 0.4 MPa and a temperature of 923 K. Symbols: experimentally observed values; lines: calculated by solving the set of Eq.7 with the reaction rates given by Eq.8 - Eq.9 for the Numaguchi model, Eq.10 - Eq.11 for the model with reactant adsorption and Eq.12 - Eq.13 for the LHHW model. The rate and equilibrium coefficients and the partial reaction orders are obtained by a weighted regression and are shown in Table 2 and Table 5. ♦ – 40 kPa inlet partial pressure of methane ($p_{CH4,in}$) and a space time of 3.36 kg_{cat} s mol_{CH4}^{-1}, ● – 80 kPa p_{CH4},in and a space time of 1.68

kg_{cat} s mol_{CH4}^{-1}, ■ – 120 kPa $p_{CH4,in}$ and a space time of 1.12 kg_{cat} s mol_{CH4}^{-1}. Top: Numaguchi model; down left: model with reactant adsorption; down right: LHHW model.

In Table 3, the residuals of the methane outlet molar flow rate, as well as those of water and carbon dioxide are shown as a function of the methane inlet partial pressure. All residual figures clearly show a systematic, parabolic trend. At the lowest and highest methane inlet partial pressures, the conversion is overestimated by the Numaguchi model, i.e., the reactant and product outlet molar flow rates are respectively underestimated and overestimated. The overestimation of the methane conversion at the lowest methane inlet partial pressures can be explained by the lack of competitive adsorption with water in the model, which becomes especially evident at the highest water inlet partial pressures, see Figure 4. In this region, including adsorption phenomena would alter the methane partial pressure dependence. At the highest methane inlet partial pressures, the same reasoning can be made. In this region, including the competitive adsorption would lower the methane consumption rate and, hence, its conversion.

Finally, the normal probability plots of the outlet molar flow rates of methane, carbon monoxide and carbon dioxide are shown in Table 4. The ordered residuals of methane and carbon dioxide clearly exhibit two tails at the highest and lowest theoretical quantile values, indicating a critical deviation from normally distributed residuals, as reflected in the corresponding, low R^2 values. This behavior could be expected due to the ill-fitting of the model as depicted in the performance curves and residual figures. The normal probability plot of carbon monoxide shows no prominent deviations.

In summary, the Numaguchi model misses essential features to describe the experimentally observed trends in our data set and, hence, is located in the underparameterized region in Figure 2.

Table 3. Residual figure of the outlet molar flow rate of methane, water and carbon dioxide as a function of the methane inlet partial pressure for the isothermal regression at a total pressure of 0.4 MPa and a temperature of 923 K, of the Numaguchi model, the model with reactant adsorption and the LHHW model. The residuals are calculated by solving the set of Eq.7 with the reaction rates given by Eq.8 - Eq.9 for the Numaguchi model, Eq.10 - Eq.11 for the model with reactant adsorption and Eq.12 - Eq.13 for the LHHW model. The rate and equilibrium coefficients and the partial reaction orders are obtained by a weighted regression and are shown in Table 2 and Table 5.

	Numaguchi model	Model with reactant adsorption	LHHW model
CH_4	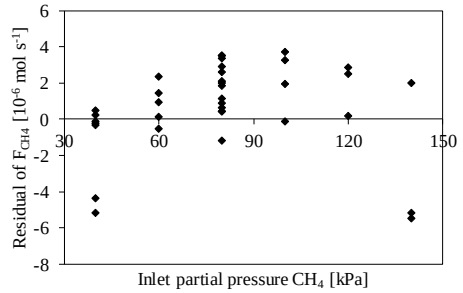	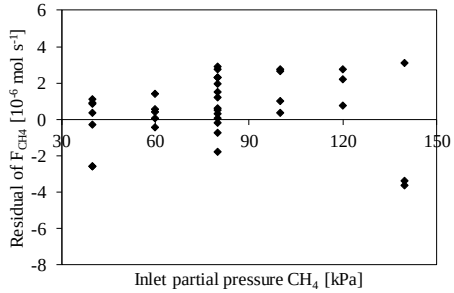	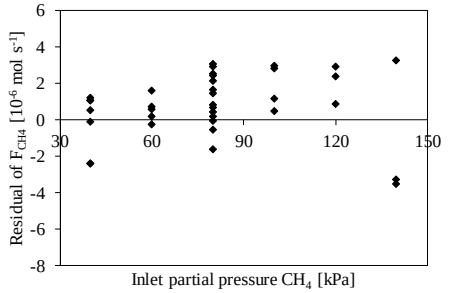
H_2O	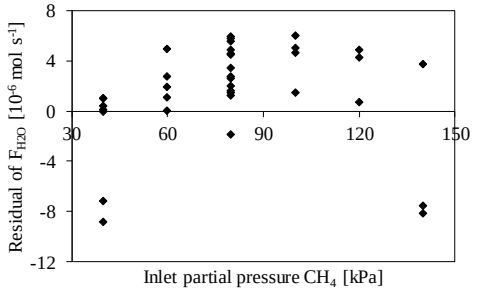	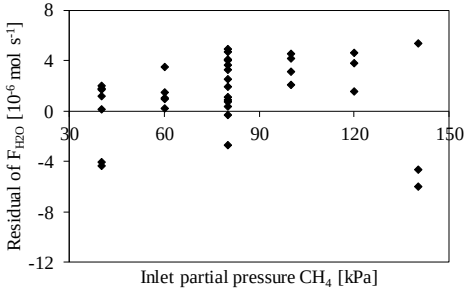	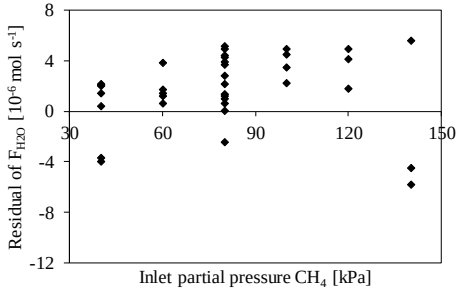
CO_2	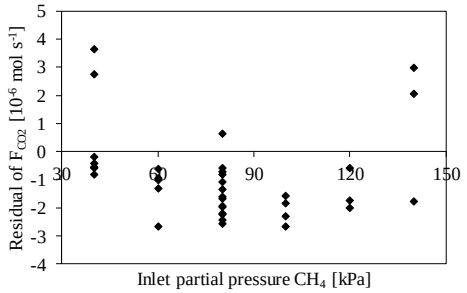	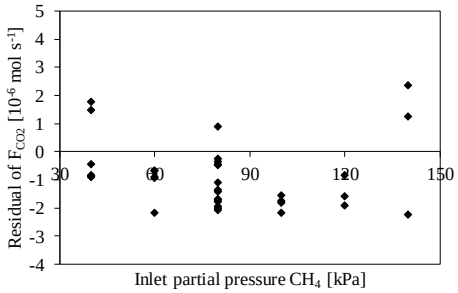	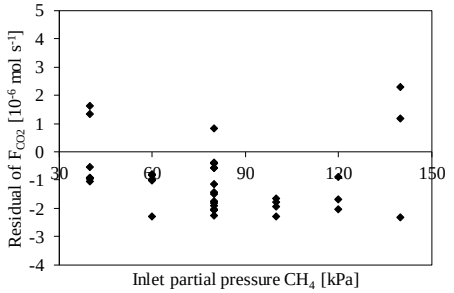

Table 4. Normal probability plot of the residuals of the outlet molar flow rate of methane, carbon monoxide and carbon dioxide for the isothermal regression at a total pressure of 0.4 MPa and a temperature of 923 K, of the Numaguchi model, the model with reactant adsorption and the LHHW model. The residuals are calculated by solving the set of Eq.7 with the reaction rates given by Eq.8 - Eq.9 for the Numaguchi model, Eq.10 - Eq.11 for the model with reactant adsorption and Eq.12 - Eq.13 for the LHHW model. The rate and equilibrium coefficients and the partial reaction orders are obtained by a weighted regression and are shown in Table 2 and Table 5.

	Numaguchi model	Model with reactant adsorption	LHHW model
CH_4	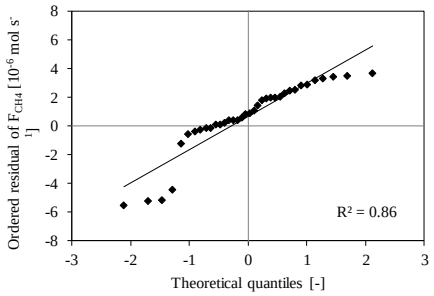	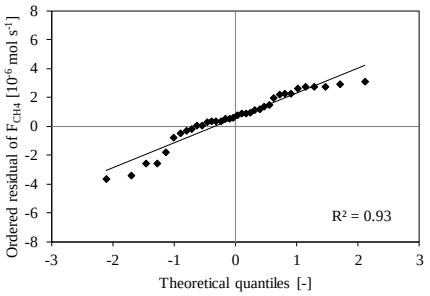	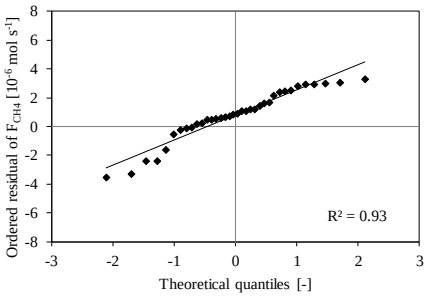
CO	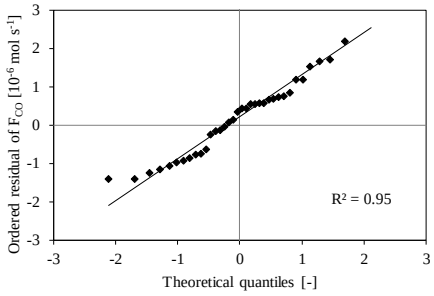	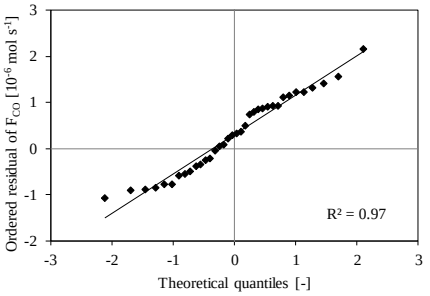	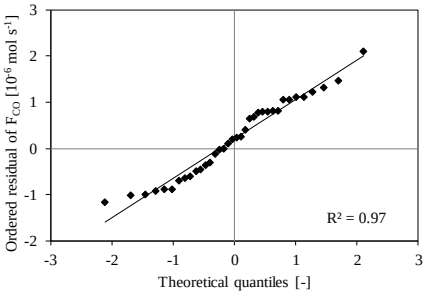
CO_2	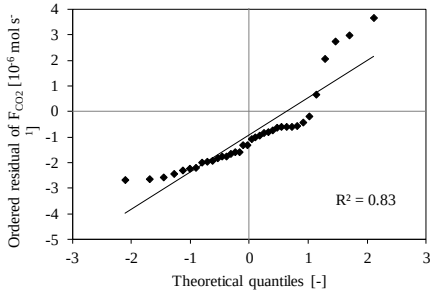	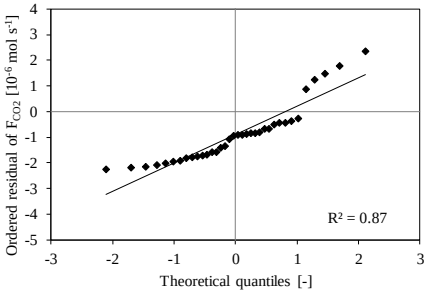	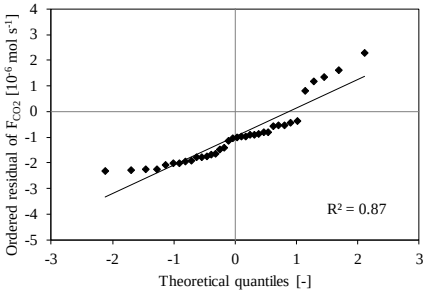

2. Relevance of reactant adsorption

Description and construction

The assessment of the Numaguchi model and the experimental data indicated clearly that including competitive adsorption effects is essential to improve the model performance. Reactant adsorption is, hence, incorporated in the next iteration of the methodology, see alternative ② in Figure 3 which contains both gas phase and surface species, and steps (5) to (8) in Table 1 [35,38-40,51]. The adsorption and desorption of methane and water are assumed to be quasi-equilibrated, based on the reasoning that methane dissociation is the most demanding and, hence, rate-determining step. It is generally agreed that, at typical reforming reactions, the surface reforming reaction is far from equilibrium, even though reactant adsorption could co-determine the rate in a certain range of experimental conditions. A thorough analysis of the rate-limiting and –inhibiting steps and species would require a degree of (thermodynamic) rate control and microkinetic assessment [52]. The products, i.e., hydrogen, carbon monoxide and carbon dioxide, are assumed to desorb as part of the surface reaction.

In our approach, the reactants are assumed to adsorb molecularly, to limit the complexity of the model. It can be reasonably expected that, in reality, methane and water will dissociate on the surface with the formation of carbon, CH_i^* (i=1,2,3), O*, OH* and hydrogen, see for example the work of Sprung et al. [35]. As a result, this model will not be able to describe the true surface coverages, yet it will allow to account for competition between adsorbed species, which is the essential feature that is being assessed in this iteration.

The rate expressions of the reforming (7) and WGS reaction (8) are consequently written in terms of the partial pressures of the gas phase species. By accounting for the adsorption equilibria and the active site balance to eliminate the concentration of free sites, this leads to the final rate expressions presented by Eq.10 and Eq.11. K_{CH4} and K_{H2O} are the methane and

water adsorption equilibrium coefficients, k_{3+} and k_{4+} the forward rate coefficients of the reforming (7) and WGS reaction (8), z is the number of adjacent active sites in case of a reaction requiring two active sites [20], C_{tot} the total concentration of active sites, K_{SMR} and K_{WGS} are the equilibrium coefficients of the global reforming, see (1), and the WGS reaction, see (2). The forward rate coefficient, z and C_{tot} are grouped to form a so-called composite rate coefficient. The exponent two in the denominator of r_3 accounts for two species reacting in the rate-determining step. The corresponding exponent of r_4 is one because the product carbon monoxide is not considered to adsorb (vide infra). This model is referred to as the *model with reactant adsorption*.

$$r_3 = \frac{k_3 z C_{tot} K_{CH_4} K_{H_2O} \left[p_{CH_4} p_{H_2O} - \frac{p_{CO} p_{H_2}^3}{K_{SMR}} \right]}{\left(1 + K_{CH_4} p_{CH_4} + K_{H_2O} p_{H_2O}\right)^2} = \frac{k_3^{comp} K_{CH_4} K_{H_2O} \left[p_{CH_4} p_{H_2O} - \frac{p_{CO} p_{H_2}^3}{K_{SMR}} \right]}{\left(1 + K_{CH_4} p_{CH_4} + K_{H_2O} p_{H_2O}\right)^2} \qquad \text{Eq.10}$$

$$r_4 = \frac{k_4 C_{tot} K_{H_2O} \left[p_{CO} p_{H_2O} - \frac{p_{CO_2} p_{H_2}}{K_{WGS}} \right]}{1 + K_{CH_4} p_{CH_4} + K_{H_2O} p_{H_2O}} = \frac{k_4^{comp} K_{H_2O} \left[p_{CO} p_{H_2O} - \frac{p_{CO_2} p_{H_2}}{K_{WGS}} \right]}{1 + K_{CH_4} p_{CH_4} + K_{H_2O} p_{H_2O}} \qquad \text{Eq.11}$$

Model and parameter estimates assessment and discussion

The regression of the model with reactant adsorption was globally significant ($F_{s,calc} = 1.06\ 10^4 > F_{s,tab} = 2.42$). Despite the addition of the adsorption of methane and water, the model remains inadequate on a statistical basis ($F_{a,calc} = 1.62 > F_{a,tab} = 1.49$). Nevertheless, the rather small $F_{a,calc}$ value indicates that this model will not perform that poor after all and, at least, much better than the Numaguchi model, see Figure 4. The performance curve will be discussed in the next section. The parameter estimates and their 95 % confidence intervals are presented in Table 5.

Table 5. Parameter estimates and the corresponding 95 % confidence intervals for the model with reactant adsorption and the LHHW model. # = non-significant parameter.

	95 % confidence intervals		units
	model with reactant adsorption[a]	LHHW model[b]	
K_{CH_4}	27.1 ± 4.5	26.6 ± 4.0	MPa^{-1}
K_{H_2O}	11.9 ± 2.2	11.9 ± 2.0	MPa^{-1}
k_3^{comp}	11.9 ± 2.2	1.66 ± 0.12	$mol\,s^{-1}\,kg_{cat}^{-1}$
k_4^{comp}	2.81 ± 0.97	1.84 ± 0.12	[a] $10^9\ mol\,s^{-1}\,kg_{cat}^{-1}\,MPa^{-1}$ [b] $10^{11}\ mol\,s^{-1}\,kg_{cat}^{-1}$
K_{CO}	/	0.240#	MPa^{-1}
K_{CO_2}	/	0.00313#	MPa^{-1}
K_{H_2}	/	0.00627#	MPa^{-1}

All parameters in the reactant adsorption model are estimated significantly different from zero with narrow confidence intervals and are not correlated. The maximum binary correlation coefficients occur between the composite rate coefficient of the reforming reaction and the water adsorption equilibrium coefficient $\left(\rho_{k_3^{comp},K_{H_2O}} = -0.92\right)$ and methane adsorption equilibrium coefficient $\left(\rho_{k_3^{comp},K_{CH_4}} = -0.93\right)$, respectively, as expected based on the presence of their product in the numerator of r_3. The adsorption equilibrium coefficients of methane and water are of the same order of magnitude. The relatively high equilibrium coefficients, imply that, in terms of surface coverages, a lot of water and methane is adsorbed on the catalyst surface. The exact surface coverages depend on the operating conditions, with an average surface coverage of 40 % of methane, 40 % of water and 20 % free sites.

The composite, forward rate coefficient of the WGS reaction, k_4^{comp}, has a very high value. This high value corresponds to a WGS equilibrium which is reached already close to the inlet of the reactor. Indeed, the experimental data set indicated a priori that the WGS reaction is close to, or at equilibrium.

Residual analysis

Including reactant adsorption in the rate expressions leads to the successful simulation of the maximum in methane conversion as a function of the water inlet partial pressure, see Figure 4. This indicates that competitive adsorption plays a kinetically relevant role, as anticipated based on the experimental data assessment and the residual analysis of the above-discussed, more simple Numaguchi model. At the highest water inlet partial pressures, the model simulates that water on the catalyst surface hinders the adsorption of methane, which decreases the reforming rate and the corresponding methane conversion. There remains a discrepancy between the model simulated values and the experimental data in the zone of competitive adsorption, possibly due to the lack of product adsorption. The correct description of the trend, i.e., the maximum in conversion, is, however, reached with the present model with reactant adsorption.

The trends in the residual figures in Table 3 have disappeared. The residuals of the outlet molar flow rate of methane, water and carbon dioxide exhibit now a more randomly distributed behavior with an average of zero and constant variance. By adding reactant adsorption, the deviations at low and high methane inlet partial pressures have been solved. Compared to the residual figures corresponding with the Numaguchi model, also the variance of the residuals decreased to half of its value for each of the responses. The normal probability plots in Table 4 confirm the previous observations and point into the direction of the assumptions made about the experimental error for methane and carbon monoxide.

The improved model performance and corresponding statistics indicate that the extended model moved from the region of underparameterization towards the region in which a balance is reached between the information contained in the experimental data set and the level of detail of the model, see step 2 in Figure 2 and Figure 3. Further improvements are still possible, as

indicated by the normal probability plot of carbon dioxide, for example by adding product adsorption.

3. Relevance of product adsorption

Description and construction

Literature typically reports low surface coverages, those of CH*, O*, H* and CO* being the most abundant ones depending on the actual surface facet and the operating conditions [35,53]. Yet, the data employed within our work on the Ni/MgO-SiO_2 catalyst, clearly indicates inhibition phenomena. It would, hence, be interesting to investigate the effect of product adsorption on the model performance. In this iteration of the systematic methodology, the molecular adsorption of the products carbon monoxide, carbon dioxide and hydrogen is also accounted for, see alternative ③ in Figure 3 with each of the five components adsorbed on the active sites, and (9) to (15) in Table 1. In line with that of the reactants, the adsorption and desorption of the products is also assumed to be in quasi-equilibrium. Both surface reactions, (11) and (12), are considered to be reversible.

The Langmuir-Hinshelwood-Hougen-Watson (LHHW) approach is followed to construct the rate expressions, see Eq.12 and Eq.13. The resulting model is referred to as the *LHHW model* in the remainder of this work. The nomenclature is similar to the terminology explained for Eq.10 and Eq.11.

$$r_3 = \frac{k_3^{comp} K_{CH_4} K_{H_2O} \left[p_{CH_4} p_{H_2O} - \frac{p_{CO} p_{H_2}^3}{K_{SMR} p_0^2} \right]}{\left(1 + K_{CH_4} p_{CH_4} + K_{H_2O} p_{H_2O} + K_{CO} p_{CO} + K_{CO_2} p_{CO_2} + K_{H_2} p_{H_2}\right)^2} \quad \text{Eq.12}$$

$$r_4 = \frac{k_4^{comp} K_{H_2O} K_{CO} \left[p_{CO} p_{H_2O} - \frac{p_{CO_2} p_{H_2}}{K_{WGS}} \right]}{\left(1 + K_{CH_4} p_{CH_4} + K_{H_2O} p_{H_2O} + K_{CO} p_{CO} + K_{CO_2} p_{CO_2} + K_{H_2} p_{H_2}\right)^2} \quad \text{Eq.13}$$

It should be noted that the LHHW models of the State-of-the-art have not been selected because of the (implicit) assumption that hydrogen is present in the feed, i.e., the inherent division by the hydrogen partial pressure, which is incompatible with not having fed hydrogen during the experimental data acquisition.

Model and parameter estimates assessment and discussion

The regression of the LHHW model was also found to be globally significant ($F_{s,calc} = 5.33\ 10^3 > F_{s,tab} = 2.06$). Adding the product adsorption did not yield an adequate model ($F_{a,calc} = 1.61 > F_{a,tab} = 1.49$).

The estimates for K_{CH4}, K_{H2O} and k_{3+}^{comp} are all statistically significant with narrow confidence intervals, see Table 5. The maximum binary correlation coefficients occur again between composite rate coefficient of the reforming reaction and the water adsorption equilibrium coefficient $\left(\rho_{k_3^{comp},K_{H_2O}} = -0.92\right)$ and methane adsorption equilibrium coefficient $\left(\rho_{k_3^{comp},K_{CH_4}} = -0.91\right)$. Moreover, the values are very close to those of the model with reactant adsorption. The value of k_4^{comp} is very high for the same reason as explained before. The two orders of magnitude difference between the composite rate coefficients of the WGS are a consequence of the different shapes of the rate equations and correspondingly different units. The adsorption equilibrium coefficients of carbon monoxide, carbon dioxide and hydrogen are not statistically significant. Several reasons can be at the origin of this result. Firstly, the products could desorb instantaneously from the catalyst surface and, hence, the corresponding adsorption coefficients are redundant to the model. Secondly, the equilibrium of the WGS reaction and the level of conversion (20-60%) can make it challenging to estimate the surface coverages and, therefore, the adsorption coefficients.

Due to the apparently redundant adsorption equilibrium coefficients, the LHHW model reduces itself to the model with reactant adsorption. Indeed, the stepwise removal of each of the non-significant adsorption equilibrium coefficients makes the reaction steps corresponding to the model shift from alternative ③ to ② in Figure 3 and, hence, the performance of both models is very similar.

Residual analysis

The performance curve in Figure 4 and the residual figures in Table 3 and Table 4 confirm the expectations of comparable performance between the model with reactant adsorption and the LHHW model. The maximum in methane conversion as a function of the water inlet partial pressure is reproduced to a very similar extent as with the reactant adsorption model. Including the adsorption of carbon monoxide, carbon dioxide and hydrogen did not further improve the model performance, as anticipated by the assessment of the parameter estimates. The systematic methodology allowed to explore the information contained in the data set and the degree of detail that could be reached within the kinetic model. The boundaries of the region in which an optimal balance between experimental information and detail accounted for in the model were reached and even crossed, by adding product adsorption. The LHHW model was overparameterized indicating that further model improvements would have to rely on other model features such as critically assessing the impact of assuming a rate-determining step. Going beyond those limits would require an even more extended data set, e.g., to be defined making use of experimental design techniques and a less idealized, microkinetic approach, i.e., by accounting for the actual reaction rates of all considered steps. As a result, the model with reactant adsorption is identified as the optimum balance between detail accounted for in the model and experimental information contained in the present data set.

Conclusions

A systematic modeling methodology, focusing in the first instance on the balance between statistical significance and physical relevance, has been further developed to guide modelers in the challenging task of kinetic modeling of chemical reactions. When developing a kinetic model, the level of detail aimed at in the model should be matched with the information that can be extracted from the experimental data set. The ultimately envisaged application of the model determines the correspondingly required level of detail and, in turn, the minimum amount of information that should be available for model development. How to find this balanced zone between experimental information and model detail is added as a new dimension to the methodology. Guidelines for identifying and avoiding under- or overparameterization are provided, such as the detection of band formation, high correlation between the model parameter estimates, the stepwise expansion of the model and the link between data analysis and model development. A case study of steam methane reforming on a Ni/MgO-SiO_2 catalyst is selected to demonstrate the successful application of the methodology. The model is regressed to an a priori determined data set, making it a an interesting and real-life example.

The systematic methodology for kinetic modeling was established as an iterative procedure, gradually extending a simple power law towards a more comprehensive Langmuir-Hinshelwood-Hougen-Watson model. Due to the missing feature of catalyst interaction, the Numaguchi model exhibited a poor performance and was not able to reproduce the maximum in methane conversion with increasing water inlet partial pressure. The model was underparameterized and had to be extended. The addition of competitive adsorption of the reactants improved the model performance significantly, while the adsorption of products did not lead to further improvements. The detail contained in the proposed Langmuir-Hinshelwood-Hougen-Watson model, with reactant and product adsorption and a total of seven model parameters was beyond the information contained in the experimental data. Hence, it was

overparameterized and reduced itself to the model with reactant adsorption and instantaneous product desorption with only four parameters. The latter model successfully simulates the trends within the experimental data set and is at the boundary of what can be reached with an idealized model.

References

1. Marin GB, Yablonsky GS. Kinetics of Chemical Reactions: Decoding Complexity. JohnWiley & Sons, Inc., 2011.
2. Stewart WE, Caracotsios M. Computer-Aided Modeling of Reactive Systems. JohnWiley & Sons, Inc., 2008.
3. McLean KAP, McAuley KB. Mathematical modelling of chemical processes—obtaining the best model predictions and parameter estimates using identifiability and estimability procedures. The Canadian Journal of Chemical Engineering. 2012;90(2):351-366.
4. Eghtesadi Z, McAuley KB. Mean-squared-error-based method for parameter ranking and selection with noninvertible fisher information matrix. AIChE Journal. 2016;62(4):1112-1125.
5. Lozano L, Marin GB, Thybaut JW. Analytical Rate Expressions Accounting for the Elementary Steps in Benzene Hydrogenation on Pt. Ind Eng Chem Res. 2017;56(45):12954-12963.
6. Thybaut JW, Marin GB. Kinetic modeling of the conversion of complex hydrocarbon feedstocks by acid catalysts. Chem Eng Technol. 2003;26(4):509-514.
7. Toch K, Thybaut JW, Marin GB. A Systematic Methodology for Kinetic Modeling of Chemical Reactions Applied to n-Hexane Hydroisomerization. AIChE Journal. 2015;61(3):880-892.

8. Anderson DM, Yun TM, Kottke PA, Fedorov AG. Comprehensive Analysis of Sorption Enhanced Steam Methane Reforming in a Variable Volume Membrane Reactor. Ind Eng Chem Res. 2017;56(7):1758-1771.
9. Hydrogen Europe - The ultimate guide to fuel cells and hydrogen technology. 2016; http://hydrogeneurope.eu/. Accessed 29/03/2018.
10. Turner JA. Sustainable Hydrogen Production. Science. 2004;305(5686):972-974.
11. Hydrogen on the rise. Nature Energy. 2016;1:16127.
12. Chaubey R, Sahu S, James OO, Maity S. A review on development of industrial processes and emerging techniques for production of hydrogen from renewable and sustainable sources. Renewable and Sustainable Energy Reviews. 2013;23:443-462.
13. Wu HJ, La Parola V, Pantaleo G, Puleo F, Venezia AM, Liotta LF. Ni-Based Catalysts for Low Temperature Methane Steam Reforming: Recent Results on Ni-Au and Comparison with Other Bi-Metallic Systems. Catalysts. 2013;3(2):563-583.
14. Hou KH, Hughes R. The kinetics of methane steam reforming over a Ni/alpha-Al2O catalyst. Chem Eng J. 2001;82(1-3):311-328.
15. Rostrup-Nielsen JR. Production of synthesis gas. Catal Today. 1993;18(4):305-324.
16. Jarosch K, El Solh T, de Lasa HI. Modelling the catalytic steam reforming of methane: discrimination between kinetic expressions using sequentially designed experiments. Chem Eng Sci. 2002;57(16):3439-3451.
17. Wildi M. Signal Extraction: Efficient Estimation, 'Unit Root'-Tests and Early Detection of Turning Points. Springer-Verlag Berlin Heidelberg, 2005.
18. Kageyama N, Devocht BR, Takagaki A, et al. Interplay of Kinetics and Thermodynamics in Catalytic Steam Methane Reforming over Ni/MgO-SiO2. Ind Eng Chem Res. 2017;56(5):1148-1158.

19. Berger RJ, Stitt EH, Marin GB, Kapteijn F, Moulijn JA. Eurokin - Chemical reaction kinetics in practice. Cattech. 2001;5(1):30-60.

20. Vannice MA. Kinetics of Catalytic Reactions. Springer, 2005.

21. Kutner MH, Nachtsheim C, Neter J, Li W. Applied Linear Statistical Models. Mcgraw-Hill Education - Europe, 2004.

22. Box GEP, Hunter JS, Hunter WG. Statistics for Experimenters: an introduction to design, data analysis, and model building. 2nd edition ed. Hoboken: John Wiley & Sons, Inc., 2005.

23. Metaxas K, Thybaut JW, Morra G, Farrusseng D, Mirodatos C, Marin GB. A Microkinetic Vision on High-Throughput Catalyst Formulation and Optimization: Development of an Appropriate Software Tool. Top Catal. 2010;53(1-2):64-76.

24. Akers WW, Camp DP. Kinetics of the methane-steam reaction. AIChE Journal. 1955;1(4):471-475.

25. Saito M, Kojima J, Iwai H, Yoshida H. The limiting process in steam methane reforming with gas diffusion into a porous catalytic wall in a flow reactor. Int J Hydrog Energy. 2015;40(29):8844-8855.

26. Wang BX, Zhu J, Lin ZJ. A theoretical framework for multiphysics modeling of methane fueled solid oxide fuel cell and analysis of low steam methane reforming kinetics. Appl Energy. 2016;176:1-11.

27. Achenbach E, Riensche E. Methane Steam Reforming Kinetics for Solid Oxide Fuel-Cells. J Power Sources. 1994;52(2):283-288.

28. Leinfelder R. Reaktionskinetische Untersuchungen zur Methan-Dampf-Reformierung and Shift-Reaktion an Anoden oxidkeramischer Brennstoffzellen. Erlangen-Nürnberg: Der Technischen Fakultät, Universität Erlangen-Nürnberg; 2004.

29. Maestri M, Vlachos DG, Beretta A, Groppi G, Tronconi E. Steam and dry reforming of methane on Rh: Microkinetic analysis and hierarchy of kinetic models. J Catal. 2008;259(2):211-222.

30. Wei JM, Iglesia E. Isotopic and kinetic assessment of the mechanism of reactions of CH4 with CO2 or H2O to form synthesis gas and carbon on nickel catalysts. J Catal. 2004;224(2):370-383.

31. Donazzi A, Beretta A, Groppi G, Forzatti P. Catalytic partial oxidation of methane over a 4% Rh/alpha-Al2O3 catalyst Part II: Role Of CO2 reforming. J Catal. 2008;255(2):259-268.

32. Ross JRH, Steel MCF. Mechanism of the steam reforming of methane over a coprecipitated nickel-alumina catalyst. Journal of the Chemical Society, Faraday Transactions 1: Physical Chemistry in Condensed Phases. 1973;69(0):10-21.

33. Numaguchi T, Kikuchi K. Intrinsic Kinetics and Design Simulation in a Complex-Reaction Network - Steam-Methane Reforming. Chem Eng Sci. 1988;43(8):2295-2301.

34. Khomenko AA, Apel'baum LO, Shub FS, Snagovsky YS, Temkin MI. Kinetics of the reaction of methane with water vapor and a reversible reaction of carbon monoxide hydrogenation on nickel. Kinetics and Catalysis. 1971(12):423-431.

35. Sprung C, Kechagiopoulos PN, Thybaut JW, Arstad B, Olsbye U, Marin GB. Microkinetic evaluation of normal and inverse kinetic isotope effects during methane steam reforming to synthesis gas over a Ni/NiAl2O4 model catalyst. Applied Catalysis a-General. 2015;492:231-242.

36. Tonkovich ALY, Yang B, Perry ST, Fitzgerald SP, Wang Y. From seconds to milliseconds to microseconds through tailored microchannel reactor design of a steam methane reformer. Catal Today. 2007;120(1):21-29.

37. Bodrov IM, Apel'baum LO, Temkin MI. Kinetics of the reaction of methane with steam on the surface of nickel. Kinetics and Catalysis. 1965(8):696-705.

38. Xu JG, Froment GF. Methane Steam Reforming, Methanation and Water-Gas Shift. 1. Intrinsic Kinetics. AIChE Journal. 1989;35(1):88-96.

39. Soliman MA, Adris AM, Alubaid AS, Elnashaie S. Intrinsic Kinetics of Nickel Calcium Aluminate Catalyst for Methane Steam Reforming. J Chem Technol Biotechnol. 1992;55(2):131-138.

40. Aparicio LM. Transient isotopic studies and microkinetic modeling of methane reforming over nickel catalysts. J Catal. 1997;165(2):262-274.

41. De Deken JC, Devos EF, Froment GF. Steam Reforming of Natural Gas: Intrinsic Kinetics, Diffusional Influences, and Reactor Design. *Chemical Reaction Engineering—Boston.* Vol 196: American Chemical Society 1982:181-197.

42. Rostrup-Nielsen JR, Christiansen LJ. Concepts in Syngas Manufacture. Vol 10: Imperial College Press, 2011.

43. Van der Borght K, Toch K, Galvita VV, Thybaut JW, Marin GB. Information-Driven Catalyst Design Based on High-Throughput Intrinsic Kinetics. Catalysts. 2015;5(4):1948-1968.

44. Bera T, Thybaut JW, Marin GB. Single-Event MicroKinetics of Aromatics Hydrogenation on Pt/H-ZSM22. Ind Eng Chem Res. 2011;50(23):12933-12945.

45. Thybaut JW, Marin GB. Single-Event MicroKinetics: Catalyst design for complex reaction networks. J Catal. 2013;308(0):352-362.

46. Bera T, Thybaut JW, Marin GB. Extension of the Single-Event Microkinetic Model to Alkyl Substituted Monoaromatics Hydrogenation on a Pt Catalyst. ACS Catal. 2012;2(7):1305-1318.

47. Vandegehuchte BD, Thybaut JW, Martinez A, Arribas MA, Marin GB. n-Hexadecane hydrocracking Single-Event MicroKinetics on Pt/H-beta. Appl Catal A-Gen. 2012;441:10-20.

48. Schmid-Schönbein GW, Woo SL-Y, Zweifach BW. Frontiers in Biomechanics. 1986.

49. Roses L, Campanari S, Manzolini G. 14 - Computational fluid dynamics (CFD) analysis of membrane reactors: simulation of a palladium-based membrane reactor in fuel cell micro-cogenerator system A2 - Basile, Angelo. *Handbook of Membrane Reactors.* Vol 1: Woodhead Publishing; 2013:496-531.

50. Froment GF, Bischoff KB, De Wilde J. Chemical Reactor Analysis and Design. Third edition ed: John Wiley & Sons, Inc, 2010.

51. Maier L, Schadel B, Delgado KH, Tischer S, Deutschmann O. Steam Reforming of Methane Over Nickel: Development of a Multi-Step Surface Reaction Mechanism. Top Catal. 2011;54(13-15):845-858.

52. Stegelmann C, Andreasen A, Campbell CT. Degree of Rate Control: How Much the Energies of Intermediates and Transition States Control Rates. J Am Chem Soc. 2009;131(23):8077-8082.

53. Blaylock DW, Zhu YA, Green WH. Computational Investigation of the Thermochemistry and Kinetics of Steam Methane Reforming Over a Multi-Faceted Nickel Catalyst. Top Catal. 2011;54(13-15):828-844.